Small saccades versus microsaccades: Experimental distinction and model-based unification

Petra Sinn*, Ralf Engbert

Universität Potsdam, Am Neuen Palais 10, 14469 Potsdam, Germany

Abstract

Natural vision is characterized by alternating sequences of rapid gaze shifts (saccades) and fixations. During fixations, microsaccades and slower drift movements occur spontaneously, so that the eye is never motionless. Theoretical models of fixational eye movements predict that microsaccades are dynamically coupled to slower drift movements generated immediately before microsaccades, which might be used as a criterion to distinguish microsaccades from small voluntary saccades. Here we investigate a sequential scanning task, where participants generate goal-directed saccades and microsaccades with overlapping amplitude distributions. We show that properties of microsaccades are correlated with precursory drift motion, while amplitudes of goal-directed saccades do not dependent on previous drift epochs. We develop and test a mathematical model that integrates goal-directed and fixational eye movements, including microsaccades. Using model simulations, we reproduce the experimental finding of correlations within fixational eye movement components (i.e., between physiological drift and microsaccades) but not between goal-directed saccades and fixational drift motion. These results lend support to a functional difference between microsaccades and goal-directed saccades, while, at the same time, both types of behavior may be part of an oculomotor continuum that is quantitatively described by our mathematical model.

Keywords: eye movements, visual fixation, microsaccades, mathematical model

1. Introduction

Our eyes move continuously to explore the world surrounding us, though we are mostly not aware of this fact. For inspection of stationary scenes, eye movements can be distinguished into saccades, ballistic eye movements that shift the gaze to a region of interest, and fixational periods, where almost all information processing on the fixated stimulus is achieved while the eye performs miniature or fixational movements (Ratliff and Riggs, 1950; Steinman et al., 1973; Haddad and Steinman, 1973; McCamy et al., 2014). Fixational eye movements are a superposition of three components (Ciuffreda and Tannen, 1995): (i) physiological drift, an erratic low-velocity motion, (ii) microsaccades, a ballistic high-velocity, small-amplitude movement, and (iii) tremor, a high-frequency oscillatory component (see Martinez-Conde et al., 2004; Rolfs, 2009, for a review).

Microsaccades and saccades form an oculomotor continuum (Zuber et al., 1965; Otero-Millan et al., 2013; Martinez-Conde et al., 2013). First, it is a well-established observation that microsaccades and saccades share the same kinematic properties, although their amplitudes can differ by orders of magnitude: Both are binocular and conjugate

*Corresponding author
Email addresses: sinn@uni-potsdam.de (Petra Sinn), ralf.engbert@uni-potsdam.de (Ralf Engbert)

behaviors (Ditchburn and Ginsborg, 1953) following the same linear relationship between amplitude and peak velocity (Zuber et al., 1965; Cook et al., 1966). Second, neurophysiological work showed that neural activity in the superior colliculus, the top-level oculomotor structure of the midbrain (Sparks, 2002), is the key generation mechanism for saccades (Lee et al., 1988) and microsaccades (Rolfs et al., 2008; Hafed et al., 2009; Hafed, 2011). Third, from a functional perspective, microsaccades contribute to precise relocation of gaze position in high-acuity visual tasks (Ko et al., 2010) in a very similar way as saccades, even though microsaccadic gaze relocations are strongly limited in their spatial extents to less than a degree of visual angle.

Typically, the distinction between saccades and microsaccades is based on a more or less arbitrary amplitude threshold that varies considerably across studies (see, e.g., Martinez-Conde et al., 2009, 2013, for a discussion). So far, however, no alternative criterion for the distinction between saccades and microsaccades has been proposed. Therefore, we set out to search for an alternative approach to the categorization of saccadic events. The rationale of our study is as follows. First, in a high-acuity observational task, we classify small saccades as goal-directed saccades or microsaccades. Second, we investigate statistical differences between both classes of events. Our definition of two separate saccade types would turn out to be arbitrary and useless, if statistical characteristics between both events types are indistinguishable, while reliable differences between event types would lend support to a new categorization of small saccades into subtypes.

While saccades are typically assumed to represent voluntary motor actions, microsaccades are considered as involuntary events (Yarbus, 1967). The strongest support for the involuntary nature of microsaccades comes from the statistical distribution of microsaccadic onset times, which follows an exponential distribution. The stochastic process that generates an exponential distribution is called a Poisson process which is characterized by constant probability over time for the observation of the next event (Cox and Miller, 1977). Since constant probability over time refers to complete temporal randomness, the exponential distribution of intersaccadic intervals for microsaccades lends support to an involuntary nature of this type of motor behavior. It is important to note, however, that the Poisson process might be modulated by additional processes for short inter-saccadic intervals and/or oscillatory components (Engbert, 2006; Bosman et al., 2009). In contrast to microsaccades, saccades do not produce an exponential distribution of inter-event times (Mergenthaler and Engbert, 2010). This can be taken as a statistical signature for stronger voluntary control of saccades compared to microsaccades. However, the labels *voluntary* and *involuntary* reflect interpretations rather than proven neurophysiological generating mechanisms. Therefore, we will introduce a task-dependent distinction between goal-directed saccades and microsaccades that is basically unrelated to the question of voluntary versus involuntary control.

How could both types of saccades statistically be differentiated? An elaborate theory on microsaccade generation needs to address potential interactions between drift (slow fixational movements) and microsaccades. Two peri-saccadic drift behavior have been reported. Post-saccadic drift is investigated well in larger saccades (Weber and Daroff, 1972; Bahill et al., 1978; Collewijn et al., 1988) and recently post-microsaccadic velocity of slow eye movements was reported to be increased compared to baseline velocity (Chen and Hafed, 2013).

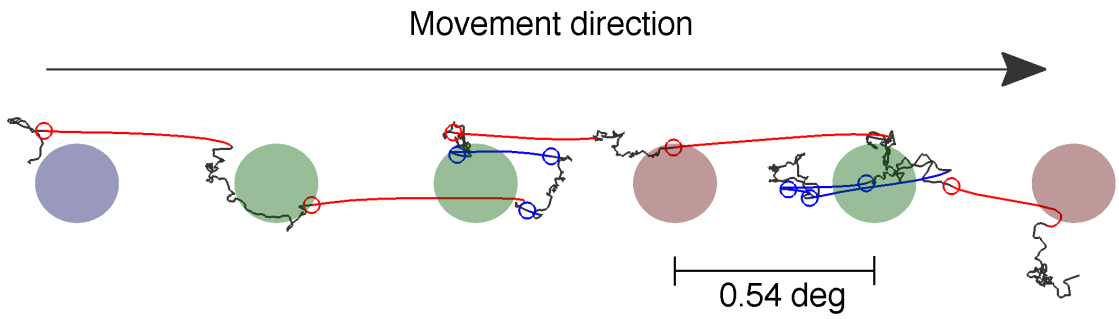

Figure 1. Experiment on simultaneous observation of small saccades and microsaccades. (*Top*) Human participants are asked to produce a series of goal-directed saccades along a color-coded chain of fixation dots. (*Bottom*) A resulting eye trace consists of small goal-directed saccades (red) and microsaccades (blue) embedded in slower drift movements (gray). The circles indicate starting points for the saccadic movements. Participants had to signal the intended saccade target by pressing a computer key mapped to the color of the target stimulus.

Pre-microsaccadic effects were reported via five lines of evidence during sustained fixation. First, the inter-individual differences in microsaccade rates were correlated to the fractal dimension of precursory drift (Engbert and Mergenthaler, 2006). Second, retinal image slip was reduced immediately before microsaccades (Engbert and Mergenthaler, 2006), which was supported in videobased systems but not for coil systems (see discussion in Chen and Hafed, 2013). Third, amplitudes of microsaccades were modulated by precursory drifts (Mergenthaler and Engbert, 2010). For small saccades during prolonged fixation, Cherici et al. (2012) found that, fourth, faster drift generates more saccadic eye movements and, fifth, less self-compensatory drift motions are related to larger saccadic amplitudes. The first three pre-microsaccadic effects were not observed for larger saccades (Mergenthaler and Engbert, 2010) and the last two effects were not investigated for larger saccades so far. Therefore, a strong (functional) interpretation of the oculomotor continuum hypothesis (Otero-Millan et al., 2013) is currently not supported by experimental data, which indicates that there might be room for a possible refinement of the definition of microsaccades.

The motivation of the current work was to investigate relationships between drift and microsaccades in a laboratory task with overlapping amplitude distributions for microsaccades and small visually guided saccades. We suspected that a difference in statistical coupling of (micro)saccades and drift exists between small saccadic movements and microsaccades. In the experimental part of the current study, we developed a high-acuity task, where human participants were instructed to generate a series of saccades (Figure 1, red color). These goal-directed (GS) saccades are aiming at a specific target stimulus, which is indicated by a participant via a color-dependent button-press. During intermediate fixations, however, spontaneous microsaccades (MS) are generated which lack an obvious movement target (Figure 1, blue color). Due to overlapping amplitudes distributions for GS and MS, our experimental paradigm permits a detailed comparison of movement statistics and, in particular, the statistical relationship between saccades and drift movements.

In general, we assumed to find stronger modulation of properties of GS (than of MS) by stimulus features (e.g., orientation of the stimulus, inter-stimulus distance). This hypothesis is based on the assumption that GS are driven by voluntarily invoked motor plans, while MS are a component of the fixational eye-movement system for controlling fixation. First, we expected longer saccade latencies for GS in short inter-stimulus distance condition compared to the long distance condition (Kalesnykas and Hallett, 1994; Adams et al., 2000). Second, the direction of GS should be toward the next stimulus element. While recent results (Ko et al., 2010) suggest that microsaccades might contribute to precise relocations of fixation position in high-acuity tasks, the distribution of microsaccadic orientations is expected to be broader than the corresponding distribution for GS. Finally, we hypothesize that GS are not statistically related to properties of slow drift movements (Mergenthaler and Engbert, 2010), while MS are expected to show such a coupling (Engbert and Mergenthaler, 2006).

Based on the experimental results, we will develop a mathematical model in the theoretical part of this study to test potential principles for the control of both saccade types observed in the experiment. Recently, we proposed an integrated computational model of fixational eye movements and microsaccades Engbert et al. (2011). In this model, drift is simulated by a self-avoiding random walk in a potential well. While the eye is in motion, the model produces movements from a self-generated activation map that can be interpreted as neural activation in the motor layer of the SC. In the model, microsaccades are triggered when the eye position enters positions related to over-critical values in the activation map.

The model was able to reproduce interactions between drift and microsaccades, in particular, the effect of reduced retinal image slip immediately before microsaccades (Engbert and Mergenthaler, 2006). In the present study, we aimed at extending the dynamical model (Engbert et al., 2011; Engbert, 2012) to include saccades to peripheral target stimuli. Therefore, we introduced a secondary potential well centered at the next target (Figure 2). The random motion in the primary potential well generates the global minimum of activation, which is either located in the primary minimum at the current fixation location or in the secondary minimum at the next target stimulus. In the first case, a microsaccade is triggered (Figure 2, MS, blue color), in the second case, a goal-directed saccade will be generated (GS, red color).

The combination of experimentation and mathematical modeling will provide new insights into the functional differences as well as similarities of microsaccades and saccades.

2. Experiment: Goal-directed saccades and microsaccades

The general strategy for our experimental design was to develop a paradigm for the observation of small saccades that are either goal-directed or fixational (i.e., microsaccades). We carried out a sequential scanning task with very short ($< 1^\circ$) inter-stimulus distances.

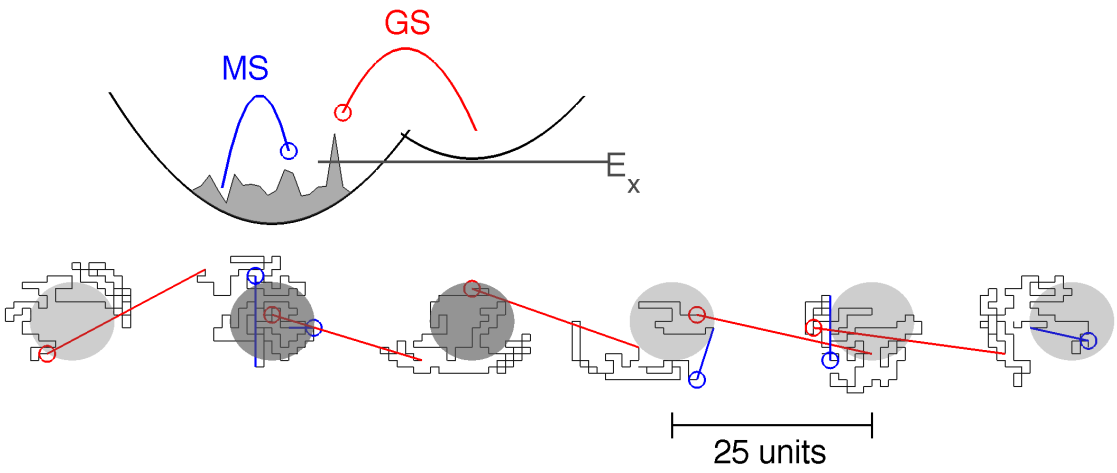

Figure 2. Dynamical model for combined generation of small goal-directed saccades and microsaccades. (*Top*) Shaded circles correspond to the row of target stimuli. In the model, the currently fixated stimulus and the next target (black dots) are considered as competing movement targets. The primary potential minimum is centered at the fixated stimulus. Drift (i.e., the self-avoiding random walk) generates fluctuations in activation, which trigger microsaccades (MS) within the primary minimum. A secondary minimum is centered at the next target stimulus. The movement target is the global minimum of both potentials, so that microsaccades (MS) and goal-directed saccades (GS) occur stochastically. (*Bottom*) A simulation example indicates the alternating behavior between goal-directed saccades (red) and microsaccades (blue) as well as random drift (gray).

2.1. Methods

2.1.1. Participants

Eighteen subjects (5 male and 13 female observers, mean age 24 years) with normal or corrected-to-normal vision took part in this study, in accordance with the ethical standards of the Declaration of Helsinki. All were naive with respect to the nature of study. Participants were invited to two sessions of 45 min duration each and were paid 14 Euros or received study credits.

2.1.2. Apparatus

Stimuli were presented on a 22inch FT/LCD monitor (refresh rate 60 Hz, resolution 1,680 x 1,050 px). Participants rested their head in a chin-rest at a viewing distance of 60 cm in a dark room. Eye movements were recorded binocularly with a video-based system (EyeLink II, SR Research, RMS $>$ 0.01°, av. accuracy 0.5°) with a sampling rate of 500 Hz and applying a heuristic filter (level 3). The experiment was programmed in Python using the VisionEgg package (Straw, 2008).

2.1.3. Task and procedure

A chain of 30 dots (diameter 3 px or 0.09°) with a distance of either 15 px (0.41°) or 20 px (0.54°) was presented on a gray background. The dots were randomly colored in dark red, dark blue, or dark green (see Figure 1). The

orientation of the chain in one of two sessions was either horizontal or vertical. To control for an expected bias toward horizontal directions in microsaccades (Engbert and Kliegl, 2003; Laubrock et al., 2005). Ten subjects started with a horizontal and eight with a vertical session. One session consisted of 60 trials with 30 trials per distance in random order. Every session started with a training task to learn the corresponding keys of three possible target colors. At the beginning and between every block consisting of 15 trials, a calibration was done. Participants started and ended every trial by pressing the space bar on a standard computer keyboard. A trial started with a fixation check. A black fixation spot was presented at the position of the first dot of the chain, either at the left side in the horizontal condition or at the top in the vertical condition. After a successful fixation for a minimum duration of 450 ms and with an accuracy within a circle of 1.2° radius around the spot, the complete chain of stimuli was made visible on the computer display. Participants were required to generate a sequence of saccades from dot to dot and a press the computer key associated to the color of the fixated stimulus element. The purpose of this key press is to provide for more fixational saccades by slowing down the performance and to have a strong criterion saccade classification (see Saccade detection).

2.1.4. Saccade detection

Saccadic movements were detected binocularly using a velocity-based algorithm (Engbert and Kliegl, 2003; Engbert and Mergenthaler, 2006) with a velocity threshold multiplier of 6 and a minimum duration of at least 6 ms above threshold. Eye blinks and saccades with amplitude larger than 1.5° were excluded from further analysis. A minimum inter-saccadic interval of 20 ms was imposed to prevent the categorization of potential overshoot components as saccadic events.

We used a standard and a conservative criterion to define small goal-directed saccades. In the standard criterion, spatial and temporal properties of all saccadic events between key press $i - 1$ and $i + 1$ were analyzed in a stepwise procedure. First, the shift in position, measured by the difference of the mean fixation position before and after the saccadic event, had to be greater than 50% of the distance between stimulus elements and directed towards the next target. Second, the temporal difference between the manual response of the participant (keypress) and the onset time of the saccadic movement had to be the minimum value across all events within the given temporal interval. Each keypress was assigned to a saccade only once. Alternatively, a conservative criterion was applied after the standard criterion that (i) controlled the correctness of the keypress via the color-coding of stimuli and (ii) avoided potentially misclassified saccades by excluding all events with directional deviations greater than ±45° from the direction to the upcoming task stimulus.

2.1.5. Box-count analysis

Drift movements were quantified by a box-count measure(Engbert and Mergenthaler, 2006). We calculated the area visited by the eye's trajectory in a fixed time interval by counting the number of squared boxes (edge length of 0.01°) needed to cover all data samples of the trajectory's epoch. The box-counts preceding all saccadic events were averaged across eyes and analyzed for five intervals of length 50 ms in time windows of 50 ms to 250 ms before

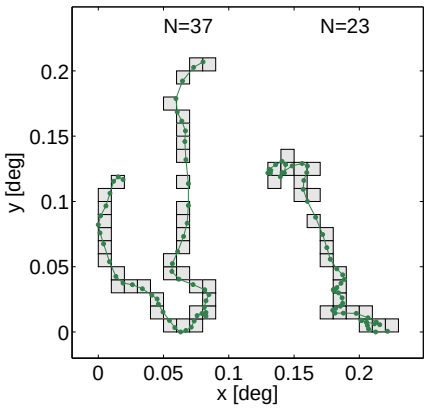

Figure 3. Schematic illustration of the box-count procedure. Two trajectories (epochs of 50 samples equivalent to 100 ms) are covered boxes of linear dimension $\Delta x = 0.01°$. The number of boxes (box-count) is given by N.

saccade onset (see Figure 3). Due to inaccuracies in the saccade-detection procedures, it cannot be excluded that data samples with high velocities are found immediately before detected saccade onsets. Therefore, we discarded data in the interval between −50 ms and saccade onset (0 ms). As an alternative measure, mean velocity was quantified by the average of the absolute local displacement between two samples within the same time intervals. The velocity was log-transformed.

2.1.6. Statistical analysis

Experimental data were analyzed statistically using linear mixed-effect models (Bates et al., 2013) in the R language of statistical computing (R Core Team, 2013). Considering the inter-individual differences, the factor participant was chosen as a random effect in all models. In general, we started with a complex model that contained all variables and the most plausible interactions. Next, we reduced this full model by excluding predictors and interactions that did not show significant effects. In the results section, we will report the reduced models only. Effects revealed to be strong, with a t-value being significant on an α-level of 5%. Standard errors (SE) are not reported, since the t-values are quotients of estimates and SEs. The dependent variables inter-saccadic intervals and amplitudes were log-transformed to better approximate normal distributions of the residuals in accordance with the statistical model.

2.2. Experimental results

2.2.1. Saccade classification

We classified 41,557 saccades as goal-directed and 15,112 saccades as microsaccades (or fixational saccades). The overall rate of saccadic events was (3.93±0.18) Hz and the ratio of goal-directed saccades to microsaccades was 2.6. The occurrence of microsaccades turned out to be unaffected to the orientation of the chain and the dot distance (Wilcox test, one-sided). Visual inspection of the angular distributions of saccadic orientations indicated an expected task-dependent distribution of goal-directed saccades (Figure 4A). For microsaccades, a task-dependent preference of

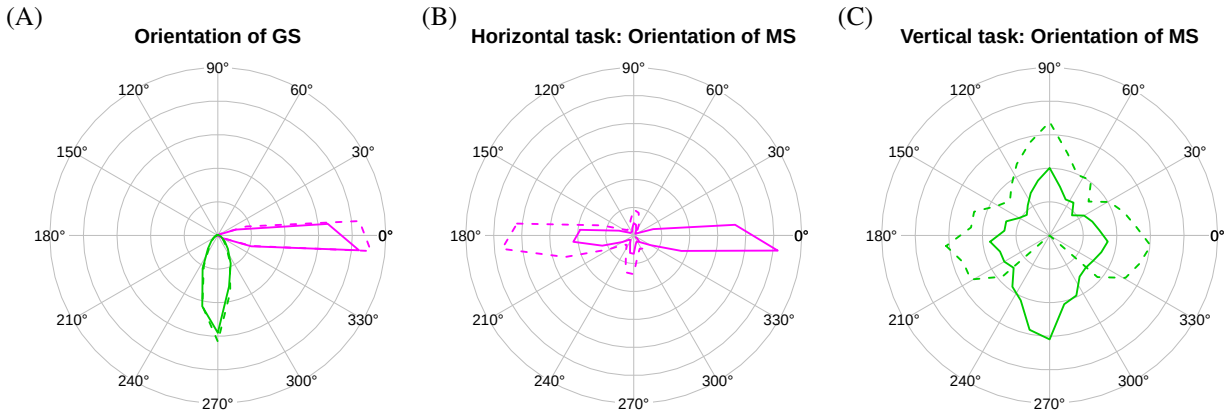

Figure 4. (A) Distribution of saccadic directions in the horizontal (pink line) and vertical (green line) orientation of the chain. (B) Distribution of microsaccade directions in the horizontal layout (pink line). (C) Results for the vertical orientation of the chain (green line). Dashed lines indicate the results corresponding to the conservative classification criterion.

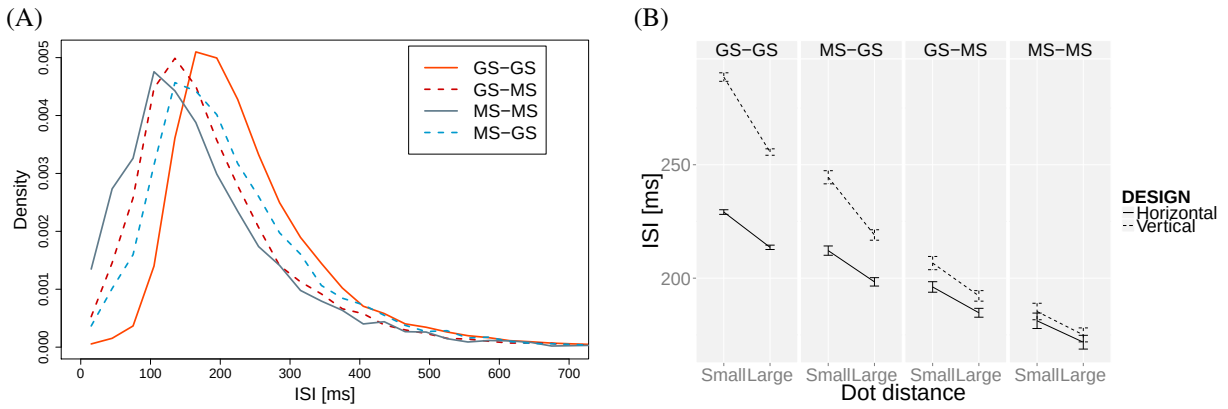

Figure 5. (A) Distribution of inter-saccadic intervals distinguished by the type of sequence. The bandwidth is 25 ms. (B) Influence of dot distance and orientation on mean inter-saccadic intervals.

orientations can be seen most clearly in the horizontal condition. The vertical task variant generates microsaccades that are more dispersed in vertical and horizontal orientations but show a preference for vertical orientations (Figure 4B, C). For the conservative criterion (see Methods 2.1), goal-directed saccades with incorrect key presses and microsaccades in task direction were excluded to avoid potential misclassifications. Results obtained from the same analysis (Figure 4, dashed lines) indicated that non-overlapping angular distributions of goal-directed saccades and microsaccades were generated. Therefore, the conservative criterion was applied whenever it was necessary to rule out effects from overlapping distributions of event types.

2.2.2. *Inter-saccadic intervals*

A plausible assumption is that saccade types can be characterized by inter-saccadic intervals (ISIs). To investigate this hypothesis, we evaluated the ISI distributions for four types of intervals defined by the type of saccadic movements

at the beginning and the end of the fixation period, respectively. Corresponding distributions of the ISIs are shown in Figure 5A. The ISI distribution between microsaccades (MS-MS) shows a shift to shorter intervals when compared to intervals between goal-directed saccades (GS-GS). The mean duration of inter-saccadic intervals for GS-GS (M = 244.0 ms) sequences is greater than the mean for MS-GS sequences (M = 217.6 ms), followed by GS-MS intervals (M = 194.7 ms) and MS-MS intervals, which turned out to be the shortest intervals on average (M = 178.1 ms; Wilcox test, $p < 10^{-15}$). This effect might be explained by the use of keypress reponses that could induce a mean prolongation of saccadic latencies. In the next step, we investigate potential unique features of goal-directed saccades and microsaccades.

It is commonly known that specific experimental manipulations can influence latencies. For example, Kalesnykas and Hallett (1994) observed a strong dependence of saccade latency on the target's eccentricity. In our experiment, the dot distance and the orientation of the chain are varied and we investigate their impact on inter-saccadic intervals. In Figure 5B, we observed that for interval types terminated by goal-directed saccades (i.e., GS-GS, MS-GS) mean ISIs decreased with increasing dot distance and increased in the vertically orientated chains compared to horizontally oriented chains. For MS terminated sequences the influence is less obvious.

Using a linear mixed-effect model for intervals from the four combinations of saccadic events, we ran a statistical analysis on the logarithm of inter-saccadic interval durations, where orientation (as two level factor), distance (as two level factor), and their interaction were considered as fixed effects (for random effects see Methods 2.1). We used a sliding difference contrast of the factors. As the first main effect, the mean durations of all intervals increased from small dot distances to large dot distances (Table 1). Interestingly, the effect of orientation of the stimulus chain turned out to be specific to GS terminated intervals. These two ISI types (i.e., MS-GS and GS-GS) show increased ISIs in the vertical compared to the horizontal orientation. Additionally, there is evidence for a statistically significant interaction, so that the orientation effect is higher for small than for large stimulus distances (Table 1, interaction term) in these two intervals. Applying the conservative criterion (data are not shown), the results are qualitatively unchanged for all sequences. Except for MS-MS sequences, the influence of dot distance turned out not to be significant; for GS-MS sequences, the factor orientation is statistically significant.

Finally, we could not find a reliable effect of target color on saccade latencies or on drift behavior. This result is in agreement with earlier work by Steinman (1965), however, an influence of target color on saccade latencies was also reported in earlier work (Perron and Hallett, 1995; Satgunam and Fogt, 2005).

2.2.3. *Pre-saccadic drift behavior*

Next, we investigated properties of the box-count measure (see Methods 2.1), of slow drift behavior immediately before saccade onsets of goal-directed and microsaccadic events. In a linear mixed-effects model, we entered the time interval (as a four-level factor) and orientation (two-level factor) as fixed effects. Additionally, the sliding difference contrast function was chosen to analyze the data via the difference between two succeeding intervals. We considered this longitudinal characteristic of the data in the random effects. As a result, the box-count turned out to be decreased

Table 1. Statistical results from linear mixed-effects modeling of the influence of stimulus distance, orientation and their interaction on the log duration of inter-saccadic intervals between combinations of goal-directed saccades and microsaccades. Δ designates the difference between the two level factors.

	GS-GS		MS-GS		GS-MS		MS-MS	
	β	t	β	t	β	t	β	t
(Intercept)	5.40	143.8	5.22	129.9	5.11	132.1	4.99	138.2
Distance Δ(Large-Small)	-0.09	18.4	-0.08	7.7	-0.05	4.3	-0.02	2.4
Orientation Δ(Vertical-Horizontal)	0.17	34.5	0.11	9.9	-0.01	0.9	-0.02	1.5
Δ(Large-Small):Δ(Vertical-Horizontal)	-0.03	3.1	-0.04	2.0	0.00	0.1	0.01	0.3

Table 2. Results from linear mixed-effect modeling of box-count and log velocity before saccadic events. A sliding difference contrast evaluates the differences between succeeding intervals. Interval 1 (-100,-50) ms, interval 2 (-150,-100) ms, interval 3 (-200,-150) ms and interval 4 (-250,-200) ms before saccadic onset.

	Box-count				log Velocity			
	GS		MS		GS		MS	
	β	t	β	t	β	t	β	t
(Intercept)	15.13	27.5	15.02	26.8	4.41	56.2	4.41	57.4
Orientation Δ(Vertical-Horizontal)	-0.61	31.6	-0.42	11.3	-0.06	17.7	-0.02	3.5
ΔBX (2-1) ms	-0.03	1.3	-0.21	4.4	-0.01	1.3	-0.03	3.2
ΔBX (3-2) ms	-0.01	0.4	0.03	0.7	0.00	0.4	0.01	0.9
ΔBX (4-3) ms	0.05	1.8	0.01	0.3	0.01	1.1	-0.00	0.1

in the vertical condition compared to the horizontal condition for both saccade types (Table 2). For microsaccades, we reproduced the earlier result (Engbert and Mergenthaler, 2006) of a significantly reduced box count $\Delta BX(2-1)$ in the time interval 2 compared to interval 1. Most importantly, such an effect was absent in goal-directed saccades. The reduction effect turned out to be reliable also for an analysis of eye velocities (Table 2) as well as for the conservative classification criterion.

2.2.4. Amplitudes

Our experiment was designed to induce small goal-directed saccades with amplitudes similar to microsaccades. In Figure 6A, the distribution of all saccadic amplitudes indicates that our experiment did not generate a bimodal distribution in the overall curve (black line). Based on the classification algorithm, we could identify two differential, but overlapping amplitude distributions for microsaccades and for goal-directed saccades. Here, microsaccades are shifted to smaller amplitudes and the distribution of amplitudes shows positive skewness. The influence of the

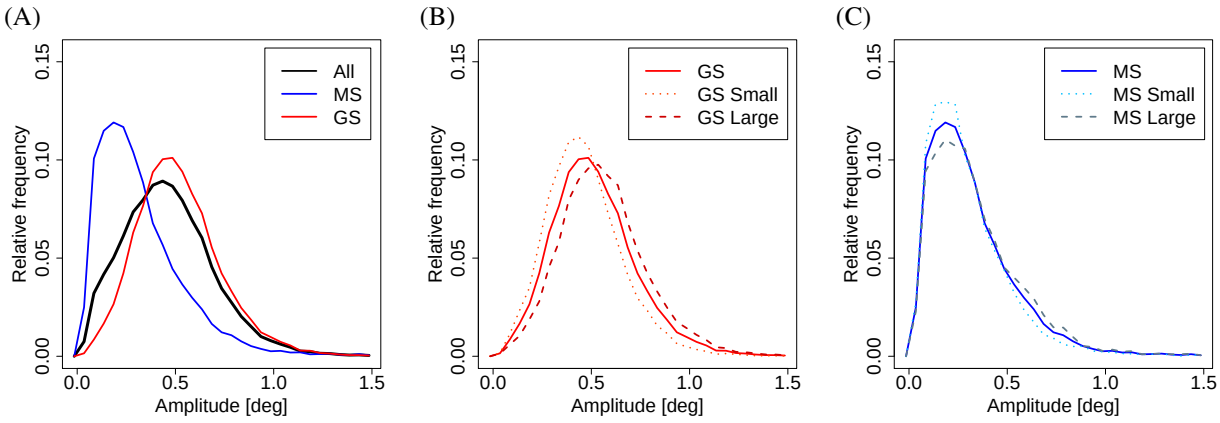

Figure 6. (A) Distribution of saccadic amplitudes. The black line shows the distribution of all saccadic events. After the classification two distinct distributions appear: one for microsaccades (blue line) and one for goal-directed saccades (red line). (B) The segregation of distance between target variation shows again a division for saccades. Small distances lead to a shift of the distribution towards smaller amplitudes (dotted lines) and larger distances cause larger amplitudes (dashed lines). (C) The influence of dot distance on microsaccade amplitudes.

inter-stimulus spacing in the experimental design is more pronounced for goal-directed saccades than for microsaccades (Figure 6B,C). We also find that goal-directed saccades as well as microsaccades are characterized by smaller amplitudes in the vertical condition than in the horizontal condition (Wilcoxtest, one-sided).

We used a linear mixed-effects model to investigate the differential influences of inter-stimulus distance and precursory box-count on saccade amplitudes. The two-level factor distance was implemented as a sliding difference contrast and box-count as the dependent variable was transformed to a rate-measure of boxes per millisecond. Separate models were computed per saccade type and orientation. The log amplitudes of goal-directed saccades turned out to depend on the stimulus distance in the horizontal as well as in the vertical condition (Table 3). In the horizontal condition, box-count has a positive impact on saccade amplitudes. However, this result was no longer reliable, when the conservative criterion was applied or when the vertical condition was analyzed. In contrast, log microsaccade amplitudes show a negative relationship to the precursory box-count. Moreover, this effect was observed for both orientations and was still highly reliable for the conservative saccade-classification criterion. We conclude that a statistically reliable effect for a negative dependence of microsaccade amplitudes on precursory box-count can be found in the experimental data, while goal-directed saccades tend to show positive, but unstable dependencies.

2.3. Interim discussion

Using a sequential saccade task with short inter-stimulus distances and two orientations of the spatial layout, we compared properties of small goal-directed saccades and microsaccades. First, we found a number of effects induced by variation of the stimulus distance. A strong influence of retinal eccentricity on the latency of saccadic movements was reported earlier (Kalesnykas and Hallett, 1994; Adams et al., 2000), where latencies decreased with increasing eccentricity below a characteristic distance and latencies increased above this distance. In agreement

Table 3. Results from linear mixed-effects modeling of log saccade amplitudes using box-count and stimulus distance as predictors.

	GS (horizontal)		GS (vertical)		MS (horizontal)		MS (vertical)	
	β	t	β	t	β	t	β	t
Standard criterion								
(Intercept)	-0.71	16.6	-0.80	20.5	-1.24	21.1	-1.40	26.8
Distance Δ(Large-Small)	0.20	42.3	0.20	28.8	0.13	7.9	0.11	7.4
Box-count	0.00	2.1	0.00	1.7	-0.02	9.4	-0.01	4.6
Conservative criterion								
(Intercept)	-0.71	16.5	-0.80	19.9	-1.51	17.6	-1.58	23.3
Distance Δ(Large-Small)	0.22	32.7	0.01	23.8	0.07	2.9	0.06	3.5
Box-count	0.00	0.2	0.00	1.7	-0.03	8.1	-0.01	5.3

with this finding, we observed that inter-saccadic intervals before and after goal-directed saccades were strongly influenced by inter-stimulus distances. In contrast, ISIs between two microsaccades tended to be independent of stimulus displays (as shown by the conservative classification criterion). However, amplitudes of both goal-directed saccades and microsaccades increased with increasing inter-stimulus distance. We could not find effects of inter-stimulus distance on drift behavior, which is in agreement with earlier findings (Hamstra et al., 2001).

Second, a strong modulation of dependent variables by the spatial orientation of the stimulus chain was found. More specifically, latencies of goal-directed saccades increased in the vertical condition, while ISIs before microsaccades appeared to be independent of orientation. Moreover, our results suggest that amplitudes were slightly reduced in the vertical condition. A possible explanation is that horizontal guidance is more frequently practiced in everyday activity (e.g., in reading). In addition to ISIs and saccade amplitudes, slow eye drifts before saccadic events were modulated by the orientation of the stimulus display. Earlier finding showed that eye drifts were modulated between a condition where a target is present compared to a condition with absent targets (St Cyr and Fender, 1969; Cherici et al., 2012). Here, we found that a vertical orientation of the scanning task produced reduced precursory box-count compared to the horizontal condition.

Third, we analyzed the mutual influences of microsaccades and physiological drift. With respect to the coupling of microsaccades to precursory drift epochs, we reproduced the effect of decreased box-count (also visible in a measure of eye velocity) immediately before an upcoming microsaccade (Engbert and Mergenthaler, 2006). In this time window (-100 ms to -50 ms), we showed that reduced drift is more likely to be followed by higher microsaccadic amplitude than on average. A previous study reported a significant positive correlation of microsaccade amplitudes and preceding box-count during time intervals of -200 ms to -100 ms (Mergenthaler and Engbert, 2010). We reproduced this finding for microsaccades, while neither the reduced box-count nor the coupling between MS and drift were found for goal-directed saccades.

The analysis of drift movements might be influenced by problems inherent to video-based eye tracking. It is known, at least on a qualitative level, that video-based data are sensitive to noise from pupil fluctuations (Wyatt, 2010; Kimmel et al., 2012), which will affect measurements of ocular drift. However, the coil system adds (i) a small additional inertia and (ii) friction to the eyeball (Frens and Van der Geest, 2002). Therefore, both techniques could produce systematic measurement biases. While video-based systems produce more observational noise, coil systems are less noisy but might add a systematic bias to the eye-movement signal, since search coils modify the eye's mechanics—an effect that might become particularly critical in low-velocity motion during fixation.

Because of these potential problems in video-based recordings, all of our analyses were based on relative changes in eye positions, not absolute values. Moreover, the robustness of our results on drift motion was tested by variation of two parameters, the spatial discretization (edge length), the temporal discretization (size of the time interval), and the influence of the cutoff value for the smallest possible ISI. The edge length for the box-counting procedure was varied from 0.01° to 0.05° in steps of 0.005°. The time window was varied from 20 ms to 100 ms. First, the reduction of pre-microsaccadic drift is robust up to an edge length of 0.05° at a fixed time window of 50 ms. The statistical significance of the coupling between amplitude and drift is stable up to 0.05° for the interval from 50 ms to 100 ms. Second, we analyzed the robustness at a fixed edge length of 0.01° with respect to variation of the duration of the temporal interval. The temporal drift modulation before microsaccades is significant up to a time window of 100 ms. The coupling of drift and microsaccade amplitudes turns out to be stable over the range from 20 ms to 100 ms. In sum, we were able to show that our numerical results are highly reliable by variation of the parameters inherent to the quantitative measures of eye drift and microsaccade detection. These posthoc analyses lend support to the interpretation that the observed interactions between drift and microsaccade amplitudes are not due to measurement error.

Recently, Chen and Hafed (2013) argued that the reduction of drift movements before microsaccades might be an artifact of video-based eyetracking. In this study, recordings by coil and video-based systems showed diverging results. While the reduced image slip was replicated with the video-based system, the recording of the coil-system did not indicate any modulation of pre-microsaccadic drift motion. Since this result was obtained from two animals (with simultaneous coil and video-based measurements in one animal), it does not invalidate our current results from video-based recordings (note that the reduced image slip before microsaccade shows considerable variability between human subjects, see Engbert and Mergenthaler, 2006), however, the results by Chen and Hafed (2013) indicate the need for more research on the issue of pre-microsaccadic drift motion. The box-count analysis is a parameter-dependent statistic that is influenced by the edge length of the boxes. Due to the lower noise level of the coil system compared to the video-based system, a systematic variation of the edge length has to be carried out to evaluate pre-microsaccadic drift for the coil system.

In addition to the general fact that the video-based methods are noisier, asymmetrical pupil dilation and constriction could also induce artifacts in gaze position for video-based systems (Drewes et al., 2012). If asymmetrical changes of the pupil induce artifical displacements of eye position, we would expect that the velocity components and, therefore, the box-count measure increase. Data indicate, however, that this effect would be limited to microsaccades

in the interval from −100 ms to −50 ms relative to microsaccade onset. Moreover, the effect is absent for goal-directed saccades.

Finally, it must be excluded that our pre-microsaccadic effect is caused by post-microsaccadic effects (Chen and Hafed, 2013) from earlier saccades. Therefore, we controlled for the potential effects of post-microsaccadic enhancement (Chen and Hafed, 2013) on pre-microsaccadic drift by increasing the minimum ISI durations for epochs included in our analysis (see Supplemental Material). As a result, excluding ISIs smaller than 150 ms decreases the overall estimation of the box-count but does not change the reduction of box-count prior microsaccades nor the almost constant baseline before goal-directed saccades.

In sum, our control analyses show that (i) pre-microsaccadic effects in the drift motion are unlikely to be caused by post-microsaccadic enhancement (Chen and Hafed, 2013) and (ii) that there is a reliable pre-microsaccadic effect specific to microsaccades but not to goal-directed saccades (Mergenthaler and Engbert, 2010).

In the next section, we will develop a computational model to investigate possible mechanisms for the difference in coupling of goal-directed saccades and microsaccades to precursory drift epochs. It will turn out that both saccade types can be reproduced in a dynamical model of eye movements during visual fixation. Moreover, the model makes specific predictions on the relationship between saccade properties and properties of the slower drift component of fixational eye movements.

3. Mathematical model

For theoretical analyses of interactions between microsaccades and drift, we used a recently proposed random-walk model (Engbert et al., 2011) for fixational eye movements under stationary viewing conditions. This model was validated based on earlier results on the statistical correlation patterns in experimental data (Engbert and Kliegl, 2004). We start with a short description of the baseline model, which is then extended to describe fixational eye movements during the sequential scanning task analyzed in the experimental part. The basic assumption for this extension is that goal-directed saccades introduce transient changes to the activation dynamics comparable to changes induced by display changes (Engbert, 2012).

3.1. Baseline model

The baseline model implements a self-avoiding random walk on a finite lattice of dimension $L \times L$ with periodic boundary conditions (Freund and Grassberger, 1992). The random walk is simulated in discrete time, where at each time step, the activation h_{ij} at current eye position (i, j) is increased by +1, i.e.,

$$h_{ij} \mapsto h_{ij} + 1 \,, \tag{1}$$

while activations at all other lattice positions $(k, l) \neq (i, j)$ decay in proportion to the current activation, i.e.,

$$h_{kl} \mapsto (1 - \epsilon) \cdot h_{kl} \,. \tag{2}$$

This basic mathematical structure is thought to implement neurophysiological processes that keep track of eye positions. To simulate visual fixation, we confined the random motion to a quadratic potential $u(i, j)$ of the form

$$u(i, j) = aL\left(\left(\frac{i - i_0}{i_0}\right)^2 + \left(\frac{j - j_0}{j_0}\right)^2\right) , \tag{3}$$

which turned out to reproduce the correlation structure (Engbert et al., 2011) with positively correlated movement increments on a short time scale (i.e., persistence) and negatively correlated increments on a longer time scale (anti-persistence). The potential well, with steepness a, is symmetric with respect to the center of intended fixation area (i_0, j_0) and confines the drift movement's excursion to a limited neighborhood of (i_0, j_0). Most recent findings lend support to the theoretical assumption of a (discrete) fixation map located in entorhinal cortex (Stensola et al., 2012; Killian et al., 2012). Activation of such a map could provide the necessary input for the superior colliculus (SC) activation generated by (Equation 1). In the SC, the sum of self-generated activation $\{h_{ij}\}$ and the potential $u(i, j)$ give rise to the movement potential $E(i, j)$, i.e.,

$$E(i, j) = h_{ij} + u(i, j) , \tag{4}$$

that drives the fixational movements in our model. As long as the numerical value of the movement potential $E(i, j)$ at the current position (i, j) is below a critical value E_{crit}, slow drift movements will be generated. The corresponding rule is that the eye will move to the minimum of the movement potential $E(i', j')$ among the four direct neighboring lattice positions (i', j'), where $i' = i \pm 1$ and $j' = j \pm 1$. In the case of a new position (i'', j'') with $E(i'', j'') \geq E_{crit}$, a microsaccadic movement is triggered with the eye position jumping to the global minimum of the movement potential. Obviously, the threshold E_{crit} controls the rate of saccadic events, since it determines how much activation needs to be accumulated before a saccadic event can be generated. For microsaccades, movement directions show a strong preference to horizontal or vertical orientations (Engbert and Kliegl, 2003; Engbert and Mergenthaler, 2006). In the model, this effect has been implemented via a secondary, oculomotor potential M of the form

$$M(i, j, i_1, j_1) = 2aL\left(\left(\frac{i - i_1}{i_0}\right)^2 + \left(\frac{j - j_1}{j_0}\right)^2\right) , \tag{5}$$

where (i_1, j_1) is the launch site of the saccade. The oculomotor potential $M(i, j, i_1, j_1)$ is added to the movement potential $E(i, j)$ before the selection of the microsaccade's target position. Thus, the global minimum of the microsaccadic movement potential

$$E_{\mathrm{MS}}(i, j) = E(i, j) + M(i, j, i_1, j_1) \tag{6}$$

is determined to select the endpoint of an upcoming microsaccade.

The baseline model (Engbert et al., 2011) was able to reproduce a range of behavioral findings on fixational eye movements and microsaccades. The two most important results were that (i) the model generated the transition from persistence to anti-persistence in the correlation patterns (Engbert and Kliegl, 2004) and that (ii) it reproduced the reduced drift movements immediately before microsaccades (Engbert and Mergenthaler, 2006).

3.2. Extension of the random-walk model

To investigate possible theoretical principles underlying the results reported in the experimental part of the current study, we propose an extension of the baseline model to develop a joint computational model of fixational eye movements (including microsaccades) and small goal-directed saccades. In an earlier paper (Engbert, 2012), the influences of sudden display changes and attentional shifts were studied within the framework of the baseline model (Engbert et al., 2011). The central assumptions are (i) that all saccadic events are triggered by the same activation-based mechanism as in the baseline model and (ii) that competition between the activation at the location of the currently fixated stimulus and the activation associated with an external stimulus determines whether the next saccade will be a goal-directed saccade or a microsaccade.

To implement such a competition, the microsaccadic movement potential $E_{\mathrm{MS}}(i, j)$, (Equation 6), is compared to an external potential $E_x = \mathrm{const}$ (Figure 2). If the external potential E_x is greater than the microsaccadic movement potential at the current position, $E_{\mathrm{MS}}(i, j) > E_x$, then a movement towards the external stimulus is generated, otherwise a microsaccade is generated according to the rules of the baseline model. Therefore, the external potential mainly influences the proportion of microsaccades and saccades, so that for high values E_x microsaccades will be more likely to occur than goal-directed saccades. With respect to the saccadic endpoint, we assume that the microsaccades target the global minimum of $E_{\mathrm{MS}}(i, j)$, while the goal-directed saccades will show landing positions randomly with conditional probability

$$P(i, j|i_1, j_1) \propto E_{\mathrm{MS}}(i, j, i_1, j_1)^{-4} \,. \tag{7}$$

Additionally, some principles of post-saccadic behavior (i.e., mechanisms of dynamical changes induced by saccade execution) had to be implemented. First, we introduce a transient change of the potential that was successfully implemented in a model for microsaccades occurring after attentional shifts (Engbert, 2012). Such a transient change is obtained by multiplying the potential $E(i, j)$ with a time-dependent factor $a_P(t)$ of the form

$$a_P(t) = \frac{1}{1 + \lambda_1 \exp(-\rho_1 t^2)} \,, \tag{8}$$

which transiently reduces the slope of the potential (Figure 7A). Second, we introduce saccadic inhibition (Engbert and Kliegl, 2003) by assuming that the threshold E_{crit} triggering saccadic events is transiently increased immediately after any type of saccadic event (Figure 7B) following the equation

$$b_{crit}(t) = 1 + \frac{1}{1 + \lambda_2 \exp(\rho_2 t^2)} \,. \tag{9}$$

3.3. Parameter estimation

Model parameters were estimated by comparing the distributions of inter-saccadic intervals obtained from experimental results with corresponding interval distributions from model simulations. In the extended model, ten free parameters had to be identified which determine the latencies of goal-directed saccades as well as microsaccades.

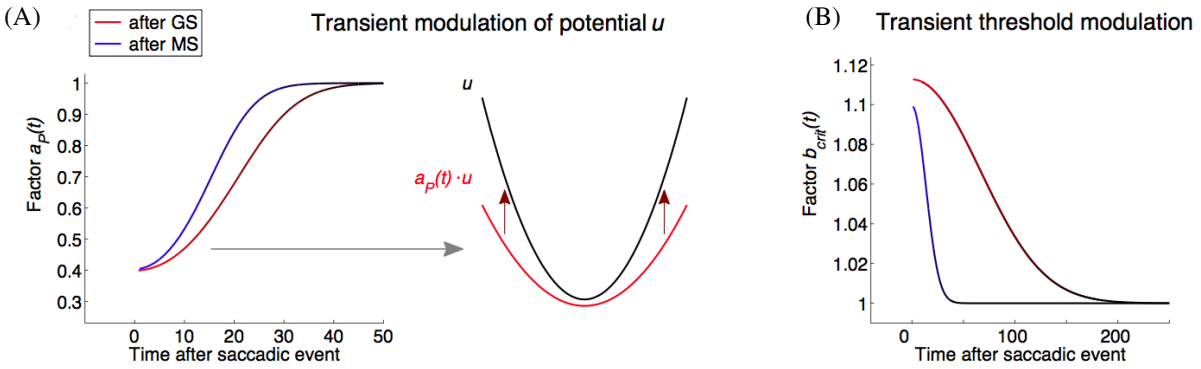

Figure 7. Functional form and schematic illustration of transient changes in model after saccadic events. (A) The time-dependent factor $a_P(t)$ for goal-directed saccades (red curve) and microsaccades (blue curve) reduces the slope of the potential $u(i, j)$. (B) The manipulation of the saccadic threshold E_{crit} due to the time-dependent coefficient b_{crit} is assumed to be weaker for goal-directed saccades than for microsaccades. The specific parameters are shown in subsection 3.3.

In the first step, we adjusted the temporal scaling by defining one iteration step as one milisecond. For the spatial scaling of the model, we chose a scaling factor of 1/25, which is equivalent to a node distance of 0.04° and a fixation area of less than 2°. Given these scaling factor, the model predicts the amplitude of microsaccades. To match the amplitude distributions observed in the experiment, a shift of 12 nodes to the right horizontal direction was assumed for goal-directed saccades.

In the second step, the distributions of ISIs were separately computed for each of the four combinations of GS and MS occurring at beginning and end of the ISI. The absolute frequency was estimated for every sequence using a bin width of 30 ms for experimental data or 30 iteration steps in the model. These two ISI distributions p_{exp} and p_{sim} are Dirichlet-multinominal distributions. Assuming that the distributions are bin-wise independent with the additional constraint that the sum equals one (due to normalization), the marginal probability distribution is β-distributed with an expectation value $\hat{E} = \frac{p}{N}$ and a variance $\text{Var} = \frac{p(N-p)}{N^2(N+1)}$, where N is the number of observations. We applied a χ^2 evaluation following the equation

$$\chi^2 = \sum \frac{(p_{\text{exp}} - p_{\text{sim}})^2}{(\text{Var}_{\text{exp}} + \text{Var}_{\text{sim}})} \tag{10}$$

and calculated the pairwise goodness of fit between the ISIs distribution of the experiment and the simulation for every GS/MS sequence type. We used a genetic algorithm (Mitchell, 1998) to estimate the parameters by minimizing the sum of χ^2 over all four possible sequences.

Estimated optimal parameter values are $E_{crit} = 7.55 \pm 0.01$, $E_x = 5.75 \pm 0.02$. The post-saccadic manipulation after saccades is descibed by $\lambda_1 = 1.51 \pm 0.1$, $\sigma_1 = (2.89 \pm 0.6) \cdot 10^{-3}$, $\lambda_2 = 7.87 \pm 0.29$, $\sigma_2 = (1.29 \pm 0.00) \cdot 10^{-4}$ and after microsaccades by $\lambda_3 = 1.48 \pm 0.12$, $\sigma_3 = (5.20 \pm 0.37) \cdot 10^{-3}$, $\lambda_4 = 9.07 \pm 0.35$, $\sigma_4 = (3.08 \pm 0.47) \cdot 10^{-3}$. Mean and error values were obtained from five separate runs of the genetic algorithm. A chain of 30 dots was simulated

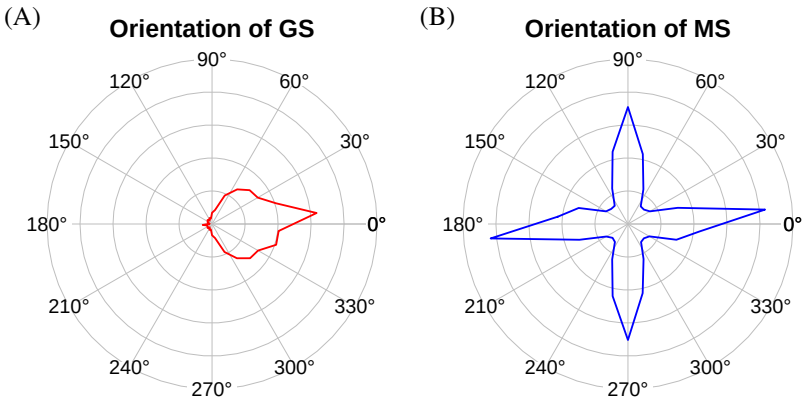

Figure 8. Saccadic orientations obtained by the extended self-avoiding random walk model. (A) Angular distribution of goal-directed saccades and (B) microsaccades.

for 18000 runs (corresponding to 120 trials × 150 virtual participants). Further parameters are the dimension of the lattice ($L = 50$) and a decay factor ($\epsilon = 0.01$). These parameters are kept constant in agreement with Engbert et al. (2011).

3.4. Modeling results

A total of 518,270 goal-directed saccades and 195,658 microsaccades were generated by numerical simulations with an overall saccade rate of (4.88±0.37) Hz and a ratio of goal-directed saccades to microsaccades of 2.6. In Figure 8, the angular distributions goal-directed saccades and microsaccades are plotted. Saccades show a strong preference to the movement direction imposed by the task. For microsaccades, however, a symmetric potential was assumed, which produces a highly symmetric occurrence for vertical and horizontal orientation.

3.4.1. Inter-saccadic intervals

In Figure 9A, we illustrate the distributions of inter-saccadic intervals of simulated and experimental data. The best fit is achieved for MS-GS, GS-MS sequences, followed by MS-MS and GS-GS sequences (see Table 4 for numerical values). Simulated and experimental distributions of the same type were not distinguishable using χ^2-test the at an α-level of 0.01.

3.4.2. Amplitudes

Next, we analyzed the amplitude distributions for saccades generated by the model. Despite the coarse spatial resolution in the numerical simulations, the model is able to reproduce the two most prominent features of amplitudes observed in the experiment: (i) The population of microsaccades is characterized by a smaller mean amplitude than the population of goal-directed saccades, and (ii) both distributions are overlapping (see Figure 9B).

Finally, we investigate the potential coupling of saccades and eye drifts, since one of the most important experimental findings of our study was the correlation between saccade amplitudes and precursory box-count. We analyzed

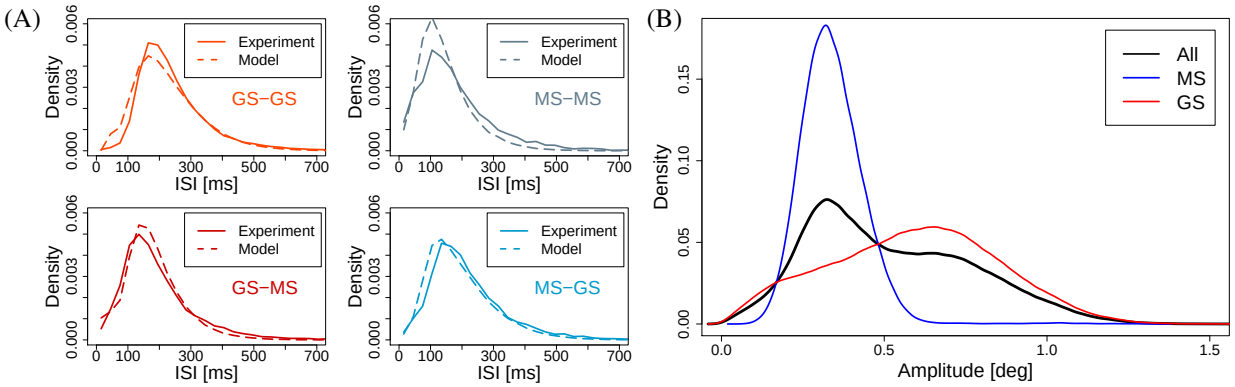

Figure 9. Numerical simulations of inter-saccadic interval distributions. (A) Inter-saccadic intervals from experimental data (solid line) and model simulations (dashed line) plotted by the four different sequences of saccade types. (B) Distributions of amplitudes for all saccadic events (black line), for goal-directed saccades (red line), and for microsaccades (blue line). For comparison, amplitudes are scaled to experimental results and kernel densities were computed.

Table 4. Mean inter-sacccadic intervals obtained from model and experiment by sequence type. The estimated χ^2 values describe the goodness-of-fit of the distributions.

	GS-GS		MS-GS		GS-MS		MS-MS	
	mean	SE	mean	SE	mean	SE	mean	SE
Model [ms]	229.6	13.7	199.7	13.3	189.7	11.0	154.6	10.3
Experiment [ms]	244.0	28.3	217.6	29.7	194.7	29.0	178.1	29.1
χ^2	*** 640		*** 517		*** 505		*** 609	

two intervals of 50 to 100 iteration steps prior to saccade onset. In good agreement with experimental results, the model does not show a dependence of saccade amplitude on previous random-walk epochs for goal-directed saccades (see Table 5). In contrast, microsaccades show a significant negative slope indicating that an increased amplitude follows decreased spatial drift behavior.

4. Discussion

In the present study, we found experimental evidence for two distinct types of saccadic events in an overlapping amplitude range. First, microsaccades were observed as a component of the eye's fixational movements, and, second, goal-directed saccades that were the result of a high-acuity sequential scanning task. We evaluated characteristics of both types of miniature saccades and concluded that they arise from different distributions of saccadic events. We proposed a computational framework that could generate both types of saccades, while, at the same time, it reproduced specific effects of coupling between microsaccades and slow fixational eye movements (physiological drift). Thus, our work lends support to specific processes of saccade-generation in the miniature range that could be integrated into

Table 5. The relationship of saccadic amplitudes and precursory box-count analyzed with a linear model. Different relationships were found for goal-directed saccades and microsaccades generated by the extended self-avoiding random-walk model.

	GS		MS	
	β	t	β	t
(Intercept)	12.089	61.0	8.650	69.6
Box-count	0.003	0.7	-0.006	2.3

the same computational model.

4.1. Main experimental findings

In general, we found that characteristics of goal-directed saccades (ISI, amplitude) are strongly modulated by external factors like inter-stimulus distance and orientation of the target, while microsaccades are less affected by these factors or even show no evidence for dependency (subsection 2.3). Among the main result in the present study, we reported that microsaccades and goal-directed saccades differ in the coupling of precursory drift motion and saccade amplitude. More specifically, we observed a reduction of drift movement and a negative relationship of the box-count and the amplitude of the following microsaccade. In contrast, amplitudes of small goal-directed saccades showed no dependence on preceding drift movements in the same time interval (Table 3 and Table 5). The effect most reliably occurs in a time window of −100 ms to −50 ms prior to microsaccades. We also discussed potential problems of the interpretation of our results, in particular, on drift movements, when using video-based eye tracking (see Interim Discussion, subsection 2.3).

For the neurophysiological interpretation, there are at least two possible pathways of saccade generation (Munoz and Everling, 2004). Reflexive saccades caused be suddenly presented stimuli (mainly investigated in the gap effect) show very short latencies. In these saccades, the incoming visual signal is presumably transformed directly into a motor command. Fixational saccades may be interpreted as reflexive or automatic saccades that are triggered by a random process producing fluctuations of activations. Steinman et al. (1967) reported a voluntary *suppression* of microsaccades, but this does not imply that microsaccade *generation* is also under voluntary control. It is important to note that a random temporal trigger mechanism does not exclude systematic modulations of microsaccades due to viewing condition (Valsecchi et al., 2007; Rolfs et al., 2008; Ko et al., 2010; Cherici et al., 2012), spatial frequency of the stimulus (Ko et al., 2010; Sinn and Engber, 2011; Hicheur et al., 2013), or attention (Hafed and Clark, 2002; Engbert and Kliegl, 2003; Kliegl et al., 2009; Valsecchi and Turatto, 2009; Hafed et al., 2011).

In other tasks or under real world conditions, it will be rather difficult to find specific functions for goal-directed and microsaccadic events in the micro-range (but see Mergenthaler and Engbert, 2010). Therefore, the typical unimodal amplitude distribution in natural scene viewing might be best described by an oculomotor continuum (Otero-Millan et al., 2013).

4.2. A mathematical model

We interpret our behavioral data with the help of a mathematical model. The baseline model (Engbert et al., 2011) introduces a dynamic neural activation field generated by a self-avoiding random walk in a symmetric potential well that simulates statistical properties of slow drift movements including their coupling to microsaccades. Saccadic events are triggered, whenever the self-generated activation is higher than a critical value. In the model, microsaccades are fast movements to the point of lowest activation. The extended model assumes an additional external potential that is selected via activation-based competition.

When we try to derive qualitative hypotheses on the statistical relation between precursory drift motion and microsaccade amplitude, we can think of two different situations of high and low box-count as a measure of eye drift. On the one hand, we suppose that a high box-count is related to a more or less uniform and flat activation field. In such a situation, almost all nodes of the lattice might be selected as possible landing positions and the probability of specific amplitudes would mainly be restricted by the current position in the potential. On the other hand, a small box-count would result in a locally increased activation pattern. In this case, we would observe a decreased number of possible landing positions very close to the current position. As a consequence, the probability for small amplitudes of microsaccades is decreased. Therefore, on average, a comparison of the situations with small and large box-counts would predict a negative correlation of box-count and microsaccade amplitude due to a reduced frequency of small microsaccades after epochs of low box-count. Moreover, goal-directed saccades are mainly affected by the position of external stimuli, with all landing positions equally likely, except for some noise-based modulation due to the current activation field.

4.3. Conclusion

Our results extend important findings on microsaccades. In early work on fixational eye movements, microsaccades were assumed to be corrective for displacements caused by drift (Ratliff and Riggs, 1950; Ditchburn and Ginsborg, 1953; Ginsborg, 1953; Cherici et al., 2012) or microsaccades and drift were found to be comparably corrective (St Cyr and Fender, 1969). Our theoretical model suggests new mechanisms how the overall task demands could induce effects on the level of the statistical properties of and the coupling between slow drifts and microsaccades.

Acknowledgments

This work was funded by Deutsche Forschungsgemeinschaft via Research Group 868 “Computational Modeling of Behavioral, Cognitive, and Neural Dynamics” (Grant EN 471/3 to R.E.).

References

Adams, M., Wood, D., Carpenter, R., 2000. Expectation acuity: the spatial specificity of the effect of prior probability on saccadic latency. The Journal of Physiology 527 (Suppl), 140P–141P.

Bahill, A. T., Hsu, F. K., Stark, L., 1978. Glissadic overshoots are due to pulse width errors. Archives of Neurology 35 (3), 138–142.

Bates, D., Maechler, M., Bolker, B., Walker, S., 2013. lme4: Linear mixed-effects models using Eigen and S4. R package version 1.0-5.

Bosman, C. A., Womelsdorf, T., Desimone, R., Fries, P., 2009. A microsaccadic rhythm modulates gamma-band synchronization and behavior. The Journal of Neuroscience 29 (30), 9471–9480.

Chen, C.-Y., Hafed, Z. M., 2013. Postmicrosaccadic enhancement of slow eye movements. The Journal of Neuroscience 33 (12), 5375–5386.

Cherici, C., Kuang, X., Poletti, M., Rucci, M., 2012. Precision of sustained fixation in trained and untrained observers. Journal of Vision 12 (6), 31.

Ciuffreda, K. J., Tannen, B., 1995. Eye movement basics for the clinician. Vol. 18. Mosby St. Louis.

Collewijn, H., Erkelens, C. J., Steinman, R., 1988. Binocular co-ordination of human horizontal saccadic eye movements. The Journal of Physiology 404 (1), 157–182.

Cook, G., Stark, L., Zuber, B., 1966. Horizontal eye movements studied with the on-line computer. Archives of Ophthalmology 76 (4), 589–595.

Cox, D. R., Miller, H. D., 1977. The theory of stochastic processes. Vol. 134. CRC Press.

Ditchburn, R., Ginsborg, B., 1953. Involuntary eye movements during fixation. The Journal of Physiology 119 (1), 1–17.

Drewes, J., Masson, G. S., Montagnini, A., 2012. Shifts in reported gaze position due to changes in pupil size: Ground truth and compensation. In: Proceedings of the Symposium on Eye Tracking Research and Applications. ACM, pp. 209–212.

Engbert, R., 2006. Microsaccades: A microcosm for research on oculomotor control, attention, and visual perception. Progress in Brain Research 154, 177–192.

Engbert, R., 2012. Computational modeling of collicular integration of perceptual responses and attention in microsaccades. The Journal of Neuroscience 32 (23), 8035–8039.

Engbert, R., Kliegl, R., 2003. Microsaccades uncover the orientation of covert attention. Vision Research 43 (9), 1035–1045.

Engbert, R., Kliegl, R., 2004. Microsaccades keep the eyes' balance during fixation. Psychological Science 15 (6), 431–431.

Engbert, R., Mergenthaler, K., 2006. Microsaccades are triggered by low retinal image slip. Proceedings of the National Academy of Sciences of the U.S.A. 103 (18), 7192–7197.

Engbert, R., Mergenthaler, K., Sinn, P., Pikovsky, A., 2011. An integrated model of fixational eye movements and microsaccades. Proceedings of the National Academy of Sciences of the U.S.A. 108 (39), E765–E770.

Frens, M., Van der Geest, J., 2002. Scleral search coils influence saccade dynamics. Journal of Neurophysiology 88 (2), 692–698.

Freund, H., Grassberger, P., 1992. The red queen's walk. Physica A: Statistical Mechanics and its Applications 190 (3), 218–237.

Ginsborg, B., 1953. Small voluntary movements of the eye. The British Journal of Ophthalmology 37 (12), 746.

Haddad, G. M., Steinman, R. M., 1973. The smallest voluntary saccade: implications for fixation. Vision Research 13 (6), 1075–IN6.

Hafed, Z. M., 2011. Mechanisms for generating and compensating for the smallest possible saccades. European Journal of Neuroscience 33 (11), 2101–2113.

Hafed, Z. M., Clark, J. J., 2002. Microsaccades as an overt measure of covert attention shifts. Vision Research 42 (22), 2533–2545.

Hafed, Z. M., Goffart, L., Krauzlis, R. J., 2009. A neural mechanism for microsaccade generation in the primate superior colliculus. Science 323 (5916), 940–943.

Hafed, Z. M., Lovejoy, L. P., Krauzlis, R. J., 2011. Modulation of microsaccades in monkey during a covert visual attention task. The Journal of Neuroscience 31 (43), 15219–15230.

Hamstra, S., Sinha, T., Hallett, P., 2001. The joint contributions of saccades and ocular drift to repeated ocular fixations. Vision Research 41 (13), 1709–1721.

Hicheur, H., Zozor, S., Campagne, A., Chauvin, A., 2013. Microsaccades are modulated by both attentional demands of visual discrimination task and background noise. Journal of Vision 13 (13:18), 1–20.

Kalesnykas, R., Hallett, P., 1994. Retinal eccentricity and the latency of eye saccades. Vision Research 34 (4), 517–531.

Killian, N. J., Jutras, M. J., Buffalo, E. A., 2012. A map of visual space in the primate entorhinal cortex. Nature 491 (7426), 761–764.

Kimmel, D. L., Mammo, D., Newsome, W. T., 2012. Tracking the eye non-invasively: simultaneous comparison of the scleral search coil and optical tracking techniques in the macaque monkey. Frontiers in Behavioral Neuroscience 6.

Kliegl, R., Rolfs, M., Laubrock, J., Engbert, R., 2009. Microsaccadic modulation of response times in spatial attention tasks. Psychological Research 73 (2), 136–146.

Ko, H.-k., Poletti, M., Rucci, M., 2010. Microsaccades precisely relocate gaze in a high visual acuity task. Nature Neuroscience 13 (12), 1549–1553.

Laubrock, J., Engbert, R., Kliegl, R., 2005. Microsaccade dynamics during covert attention. Vision Research 45 (6), 721–730.

Lee, C., Rohrer, W. H., Sparks, D. L., et al., 1988. Population coding of saccadic eye movements by neurons in the superior colliculus. Nature 332 (6162), 357–360.

Martinez-Conde, S., Macknik, S. L., Hubel, D. H., 2004. The role of fixational eye movements in visual perception. Nature Reviews Neuroscience 5 (3), 229–240.

Martinez-Conde, S., Macknik, S. L., Troncoso, X. G., Hubel, D. H., 2009. Microsaccades: a neurophysiological analysis. Trends in Neurosciences 32 (9), 463–475.

Martinez-Conde, S., Otero-Millan, J., Macknik, S. L., 2013. The impact of microsaccades on vision: towards a unified theory of saccadic function. Nature Reviews Neuroscience 14 (2), 83–96.

McCamy, M. B., Otero-Millan, J., Di Stasi, L. L., Macknik, S. L., Martinez-Conde, S., 2014. Highly informative natural scene regions increase microsaccade production during visual scanning. The Journal of Neuroscience 34 (8), 2956–2966.

Mergenthaler, K., Engbert, R., 2010. Microsaccades are different from saccades in scene perception. Experimental Brain Research 203 (4), 753–757.

Mitchell, M., 1998. An introduction to genetic algorithms. MIT press.

Munoz, D. P., Everling, S., 2004. Look away: the anti-saccade task and the voluntary control of eye movement. Nature Reviews Neuroscience 5 (3), 218–228.

Otero-Millan, J., Macknik, S. L., Langston, R. E., Martinez-Conde, S., 2013. An oculomotor continuum from exploration to fixation. Proceedings of the National Academy of Sciences of the U.S.A. 110 (15), 6175–6180.

Perron, C., Hallett, P., 1995. Saccades to large coloured targets stepping in open fields. Vision Research 35 (2), 263–274.

R Core Team, 2013. R: A Language and Environment for Statistical Computing. R Foundation for Statistical Computing, Vienna, Austria, R version 3.0.2.

Ratliff, F., Riggs, L. A., 1950. Involuntary motions of the eye during monocular fixation. Journal of Experimental Psychology 40 (6), 687.

Rolfs, M., 2009. Microsaccades: small steps on a long way. Vision Research 49 (20), 2415–2441.

Rolfs, M., Kliegl, R., Engbert, R., 2008. Toward a model of microsaccade generation: The case of microsaccadic inhibition. Journal of Vision 8 (11), 5.

Satgunam, P., Fogt, N., 2005. Saccadic latencies for achromatic and chromatic targets. Vision Research 45 (27), 3356–3364.

Sinn, P., Engber, R., 2011. Saccadic facilitation by modulation of microsaccades in natural backgrounds. Attention, Perception, & Psychophysics 73 (4), 1029–1033.

Sparks, D. L., 2002. The brainstem control of saccadic eye movements. Nature Reviews Neuroscience 3 (12), 952–964.

St Cyr, G. J., Fender, D. H., 1969. The interplay of drifts and flicks in binocular fixation. Vision Research 9 (2), 245–265.

Steinman, R. M., 1965. Effect of target size, luminance, and color on monocular fixation. Journal of the Optical Society of America 55 (9), 1158–1164.

Steinman, R. M., Cunitz, R. J., Timberlake, G. T., Herman, M., 1967. Voluntary control of microsaccades during maintained monocular fixation. Science 155 (3769), 1577–1579.

Steinman, R. M., Haddad, G. M., Skavenski, A. A., Wyman, D., 1973. Miniature eye movement. Science 181 (4102), 810–819.

Stensola, H., Stensola, T., Solstad, T., Frøland, K., Moser, M.-B., Moser, E. I., 2012. The entorhinal grid map is discretized. Nature 492 (7427), 72–78.

Straw, A. D., 2008. Vision egg: an open-source library for realtime visual stimulus generation. Frontiers in Neuroinformatics 2.

Valsecchi, M., Betta, E., Turatto, M., 2007. Visual oddballs induce prolonged microsaccadic inhibition. Experimental Brain Research 177 (2), 196–208.

Valsecchi, M., Turatto, M., 2009. Microsaccadic responses in a bimodal oddball task. Psychological Research 73 (1), 23–33.

Weber, R. B., Daroff, R. B., 1972. Corrective movements following refixation saccades: type and control system analysis. Vision Research 12 (3), 467–475.

Wyatt, H. J., 2010. The human pupil and the use of video-based eyetrackers. Vision Research 50 (19), 1982–1988.

Yarbus, A. L., 1967. Eye movements during fixation on stationary objects. In: Eye movements and vision. Springer, pp. 103–127.

Zuber, B. L., Stark, L., Cook, G., 1965. Microsaccades and the velocity-amplitude relationship for saccadic eye movements. Science 150 (3702), 1459–1460.